Investigation of the Competition between Electron and Energy Transfer in the Quenching of Aromatic Ketones in the Triplet State Using Picosecond Transient Grating Spectroscopy

Claudia Högemann and Eric Vauthey*

Institute of Physical Chemistry of the University of Fribourg, Pérolles, CH-1700 Fribourg, Switzerland

Received: April 13, 1998; In Final Form: June 16, 1998

The competition between electron transfer (ET) and triplet energy transfer (TT) in the quenching of benzophenone, xanthone, and anthraquinone in the triplet state by molecules with both a sufficiently small oxidation potential and low triplet state was investigated in the picosecond to microsecond time scales. In the longer time scale, the product distribution depends strongly on the relative exergonicity of ET and TT processes, the yield of the lower energy product being at least four times larger than that of the other product. Picosecond transient grating measurements reveal that if TT is more exergonic than ET, the TT product is predominantly formed by two sequential ET reactions, i.e., by spin-allowed back ET within the triplet geminate ion pair formed upon ET quenching. However, if ET is more exergonic than TT, no conversion from the TT product to the ET product could be detected. In this case, the product distribution in the microsecond time scale seems to reflect the competition between the two processes. When both processes are exergonic, ET appeared to be always faster than TT. This is in agreement with the severe orbital overlap requirement for TT via the Dexter exchange mechanism.

Introduction

Electron transfer (ET) and energy transfer are very important quenching processes of excited states. Singlet−singlet energy transfer and triplet−triplet energy transfer (TT) have to be distinguished. The first one, involving spin-allowed electronic transitions, proceeds mainly through the Coulombic interaction and can take place over large distances.[1] This mechanism is no longer operative in the case of TT, because of the weakness of the electric dipoles for spin-forbidden transitions. In this case, energy transfer takes place through the exchange interaction, which only requires that the spin functions of the reactants change simultaneously during the energy transfer.[2] Qualitatively, the exchange mechanism, often referred to as the Dexter mechanism, can be regarded as follows: the excited electron of the energy donor is transferred to the acceptor during the simultaneous ET from the acceptor to the donor. Contrary to the first mechanism, also referred to as the Förster mechanism, contact between the reactants is required for this electron exchange to take place. When the excited state is the singlet state, ET which requires contact or at least small distance between the reactants cannot compete efficiently with Förster energy transfer, if both processes are feasible. In this case, energy transfer will be the dominant quenching process. The situation is rather different in the case of a triplet excited state. Indeed, ET and TT show several similarities. For example, Closs and co-workers have shown that both intramolecular ET and TT rate constants decrease exponentially upon increasing the distance between the reactive groups.[3,4] Interestingly, the distance dependence of TT was found to be about two times larger than the distance dependence of ET. In the same way, the rate constants for quenching through both intermolecular ET[5−7] and TT[8−10] in solution show an asymptotic free energy dependence as those proposed by Rehm and Weller[7] and by Agmon and Levine.[11] Moreover, a decrease of the rate constant with increasing free energy, similar to that observed for ET reactions in the "Marcus inverted region",[12,13] has been reported for intramolecular TT[14,15] and also recently for intermolecular TT.[16]

These two quenching processes have been essentially studied with systems where only one process was energetically possible. What does happen when both processes are feasible? Are both processes fully independent? If they are, what are the parameters controlling this competition? The conditions required to allow both processes to take place are (1) that the free energy for photoinduced ET is negative (or at least not too positive) and (2) that the lowest triplet state of the quencher lies below that of the excited molecule. Shizuka and co-workers have investigated such systems using nanosecond flash photolysis and found that the primary quenching product was the quencher in the triplet state, which was assumed to be generated via the Dexter exchange mechanism.[17,18]

Working in the same time scale, Tinkler et al. have shown that both TT and ET products were formed in the quenching of triplet nitronaphthalene by carotenoids in methanol.[19] Here as well, both processes were assumed to occur independently. The same authors showed that only the triplet product was generated in hexane, although ET was energetically possible. To explain this difference, a higher free energy barrier for ET in hexane relative to methanol due to different solvent reorganization energies was invoked.[20] In this case as well, the triplet product was assumed to be generated through the Dexter mechanism.

We present here an investigation of the competition between ET and TT using picosecond transient grating spectroscopy. The systems studied here consist of different aromatic ketones (M) as electron acceptor, or triplet energy donor, and naphthalene derivatives as well as *N*,*N*-dimethylaniline (Q) as electron donors, or triplet energy acceptors, in acetonitrile. Redox potentials and triplet energies are listed in Table 1.

* Author to whom correspondence should be addressed. E-mail: Eric.Vauthey@unifr.ch.

10.1021/jp981810o CCC: $15.00
Published on Web 11/10/1998

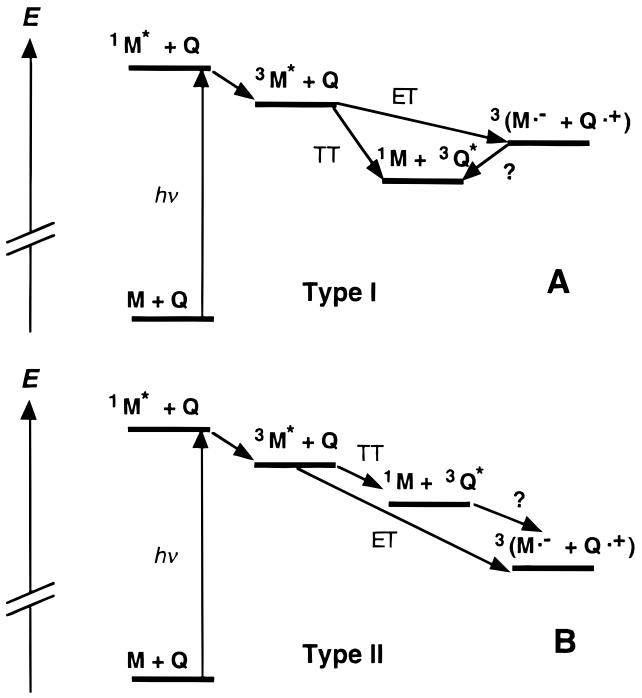

Figure 1. Possible processes with M/Q pairs for which the ET product is above (Type I pairs, A) and below the TT product (Type II pairs, B).

TABLE 1: Redox Potentials and Triplet Energies of the Various M and Q Molecules

M	E_{red}(M) (V vs SCE)	E_T(M)[50] (eV)	Q	E_{ox}(Q)[51] (V vs SCE)	E_T(Q)[50] (eV)
BP	−1.73[52]	3.0	NAP	1.72	2.65
XA	−1.65[53]	3.2	MNAP	1.53	2.60
AQ	−0.94[54]	2.7	1-MONAP	1.38	2.68
			2-MONAP	1.42	2.60
			DMA	0.71	3.0

These M/Q pairs can be classified into two types, as shown in Figure 1: pairs where the ET product lies above the TT product, such as xanthone/1-methoxynaphthalene (Type I, Figure 1A) and pairs where ET is more exergonic than TT, such as 9,10-anthraquinone/1-methoxynaphthalene (Type II, Figure 1B). For each system, absorption bands of both ^{3}M* and ^{3}Q* and of either $M^{\cdot-}$ or $Q^{\cdot+}$ lie in the spectral window of the transient grating experiment (440 nm−760 nm). This technique was preferred to the more conventional transient absorption spectroscopy because of its superior sensitivity. These experiments have been combined with photoconductivity and microsecond transient absorption measurements to establish the detailed mechanism of triplet state quenching.

Experimental Section

Apparatus. The picosecond transient grating (TG) setup has been described in details previously.[21] In brief, the third harmonic output at 355 nm of an active/passive mode-locked Q-switched Nd:YAG laser with a single amplification stage (Continuum PY61-10) was split into two parts which were recombined, both spatially and temporally, on the sample with an angle of incidence of 0.2°. The duration of the pulse was about 30 ps, and the pump energy on the sample was around 500 μJ. The remaining laser output at 1064 nm with an energy of around 12 mJ was sent along a variable optical delay line before being focused into a 25 cm long cell filled with a 70:30 (v/v) D_2O/H_2O mixture for continuum generation. The resulting white light pulses (440−760 nm) were spatially filtered and focused on the sample to a spot about 2 mm in diameter with an angle of incidence of 0.25°. The diffracted signal was passed through a cutoff filter (Schott GG400) to eliminate scattered pump light and focused in a light guide connected to the entrance of a 1/4 m imaging spectrograph (Oriel Multispec 257). As detector, a 1024 × 256 pixels water-cooled CCD camera (Oriel Instaspec IV) was used. Only spectra obtained with pump and probe pulses within a small energy range were taken into account. At each position of the delay line, the TG spectrum was averaged over 70 of such good shots.

TABLE 2: Free Energies for ET and TT and Free Ion Yields for the Various M/Q Pairs

M	Q	ΔG_{ET} (eV)	ΔG_{TT} (eV)	$\Delta G_{ET} - \Delta G_{TT}$ (eV)	Φ_{ion} (%)
BP	2-MONAP	0.15	−0.40	0.55	4
	1-MONAP	0.11	−0.32	0.43	7
XA	MNAP	−0.02	−0.60	0.62	4
	2-MONAP	−0.13	−0.60	0.47	10
	1-MONAP	−0.17	−0.52	0.35	12
	DMA	−0.84	−0.20	−0.64	82
AQ	NAP	−0.04	−0.05	0.01	6
	MNAP	−0.23	−0.10	−0.13	23
	2-MONAP	−0.34	−0.10	−0.24	70
	1-MONAP	−0.38	−0.02	−0.36	78

Free ion yields were determined using photoconductivity. The photocurrent cell has been described in detail elsewhere.[22] The system benzophenone with 0.02 M 1,2-diazabicyclo[2.2.2]-octane in MeCN, which has a free ion yield of unity,[23] was used as a standard. The measurements were made in single shot mode to prevent degradation of the solution.

The microsecond transient absorption spectra were measured using a conventional laser flash photolysis setup equipped with a Q-switched Nd:YAG laser (JK Laser model 2000). The data acquisition was made on a 500 MHz digital oscilloscope (Tektronik TDS-620A) interfaced with a personal computer.

Samples. 1,2-Diazabicyclo[2.2.2]octane (DABCO), 9,10-anthraquinone (AQ), and 2-methoxynaphthalene (2-MONAP) were purified by sublimation. Benzophenone (BP, Aldrich), naphthalene (NAP, Roth), and xanthone (XA) were twice recrystallized from ethanol. 1-Methoxynaphthalene (1-MONAP) was vacuum distilled over CaH_2 and 1-methylnaphthalene (MNAP) was first refluxed on BaO and then vacuum distilled. *N*,*N*-Dimethylaniline (DMA) was twice vacuum distilled. Acetonitrile (MeCN, UV grade) was used as such. Unless specified, all chemicals were from Fluka.

For the TG experiment, the absorbance of the sample solutions at 355 nm was around 0.15 over 1 mm, the cell thickness. For photoconductivity and transient absorption measurements, the sample absorbance over 1 cm was around 0.5 at 355 nm. All samples were deoxygenated by nitrogen bubbling. For TG and transient absorption measurements, the samples were continuously flowed. All measurements were performed at 20 °C.

Results

Free Ion Yields. The free ion yields measured by photoconductivity are listed in Table 2. The values range from 4% to about 80%, depending on the systems. The free ion yield, ϕ_{ion}, is defined as[24]

$$\Phi_{ion} = \Phi_{IP}\Phi_{sep} \quad (1)$$

where Φ_{IP} is the efficiency for ion pair formation and Φ_{sep} is the separation efficiency of the resulting geminate ion pair. If

quenching occurs through ET only, Φ_{IP} is given by

$$\Phi_{IP} = \frac{k_q \tau_0 [Q]}{k_q \tau_0 [Q] + 1} \tag{2}$$

where τ_0 is the triplet state lifetime at zero Q concentration and k_q is the quenching rate constant and is equal to

$$k_q = \frac{k_{ET} k_d}{k_{ET} + k_{-d}} \tag{3}$$

where k_d is the second-order rate constant describing the diffusional encounter of the reactant and k_{-d} is the first-order rate constant for the opposite process. With all the pairs studied, the triplet quenching was essentially diffusion controlled. Considering the lifetime of ^{3}AQ*, ^{3}BP*, and ^{3}XA*, which lies between 0.2 and 1 μs,[25] and the Q concentration of 0.1 M used in these experiments, Φ_{IP} can be expected to be unity for all pairs with $\Delta G_{ET} < 0$, if ET is the only quenching process. The separation efficiency of the geminate ion pair is given by

$$\Phi_{sep} = \frac{k_{sep}}{k_{sep} + k_{BET}^{GS}} \tag{4}$$

where k_{sep} is the rate constant for the separation of the geminate ion pair to free ions and k_{BET}^{GS} the rate constant for back ET (BET) to the neutral ground state. Since the geminate ion pair is formed in the triplet state, k_{BET}^{GS} is spin forbidden and therefore ϕ_{sep} is unity.[26,27] Consequently, if ET is the only quenching process, the ion yield should be close to unity for the pairs with $\Delta G_{ET} < 0$.

Figure 2A shows the free ion yields plotted as a function of the free energy gap between the ET and TT products, $\Delta G_{ET} - \Delta G_{TT}$. This figure indicates that the free ion yield is smaller than 10% when the TT product lies below the ET product, while it can be as high as 80% in the opposite case. With AQ/NAP and AQ/MNAP, ϕ_{ion} is smaller than expected. As discussed in more details below, triplet quenching with these systems results not only in ET and TT products, but also in the formation of a third product.

Figure 2B shows the dependence of ϕ_{ion} on the free energy for ET calculated as $\Delta G_{ET} = E_{ox}(Q) - E_{red}(M) - E_T$, where E_T is the energy of the excited state and where $E_{ox}(Q)$ and $E_{red}(M)$ are the oxidation and reduction potentials of the electron donor and acceptor, respectively. For comparison, free ion yields at [Q] = 0.1 M with M/Q pairs for which triplet quenching occurs upon ET only (ET-pairs) are also plotted. The solid line has been computed using eqs 1−4, with $k_d = 1.9 \times 10^{10}$ M^{-1} s^{-1}, $k_{-d} = 2.2 \times 10^{10}$ s^{-1},[10] [Q] = 0.1 M, $\tau_0 = 0.5$ μs and using the classical Marcus expression to calculate k_{ET}, assuming a total reorganization energy of 1.5 eV and a prefactor of 1×10^{13} s^{-1}. The agreement between the measured ion yields for ET-pairs and the calculated yields is very good. The free energy dependence of the free ion yields for the other pairs (ET/TT-pairs) exhibits a similar shape but with a shift of about 0.3 eV toward higher exergonicity. For the ET-pairs, the inflection point of the free energy dependence takes place when the energy of the ion pair is below the energy of the reactants. For the ET/TT-pairs, it appears that the inflection point occurs when the energy of the ET product becomes lower than that of the TT product. With [Q] = 0.1 M, the triplet state quenching is complete for all ET/TT pairs, independently of ΔG_{ET}. This is not the case for the ET-pairs with $\Delta G_{ET} > 0$. This shows

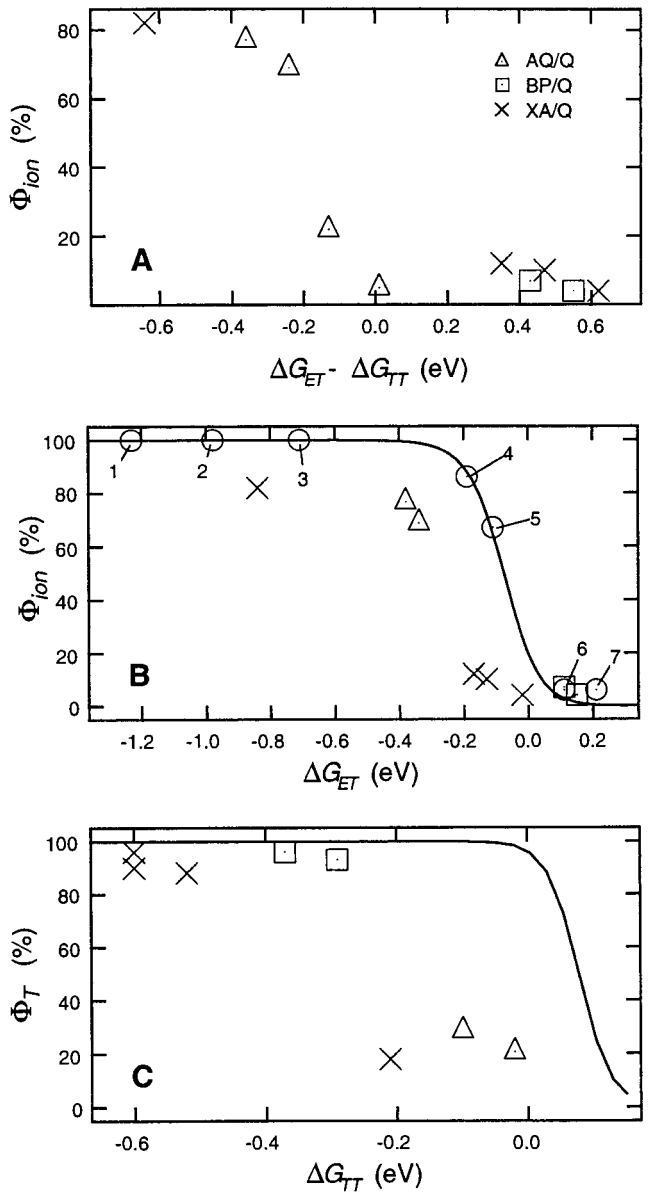

Figure 2. (A) Correlation between the free ion yields measured with AQ, BP, and XA and different quenchers ([Q] = 0.1 M) and the energy difference between the ET and TT products. (B) Correlation between the free ion yields and ΔG_{ET} for ET/TT-pairs as well as for ET-pairs with [Q] = 0.1 M (circles, 1: AQ/1,4-diaza[2,2,2]bicyclooctane;[26] 2: AQ/DMA;[26] 3: BP/1,4-diaza[2,2,2]bicyclooctane;[26] 4: tetracenequinone/1,2-dimethoxybenzene;[55] 5: BP/1,2,4-trimethoxybenzene;[34] 6: BP/1,2-dimethoxybenzene;[34] 7: BP/1,4-dimethoxybenzene[34]); the solid line is the calculated free energy dependence of the free ion yield for ET-pairs (see text). (C) Correlation between the triplet yields and ΔG_{TT} for the same pairs as in (B) and calculated free energy dependence assuming TT quenching only (solid line).

that the contribution of TT to triplet quenching is dominant for the ET/TT-pairs with $\Delta G_{ET} > 0$.

Figure 2C shows the triplet yields for the ET/TT-pairs plotted as a function of the free energy for TT, calculated as $\Delta G_{TT} = E_T(M) - E_T(Q)$, where $E_T(M)$ and $E_T(Q)$ are the triplet energies of the energy donor and of the energy acceptor, respectively. The triplet yields have been calculated as $\phi_T = 1 - \phi_{ion}$, since for these systems only ET and TT products have been observed (vide infra). High ϕ_T are measured for $\Delta G_{TT} < -0.3$ eV, while for less exergonic TT, the triplet yield is smaller than 20%. The continuous line on this figure is the triplet yield calculated in a similar fashion to the curve in Figure 2B but using the

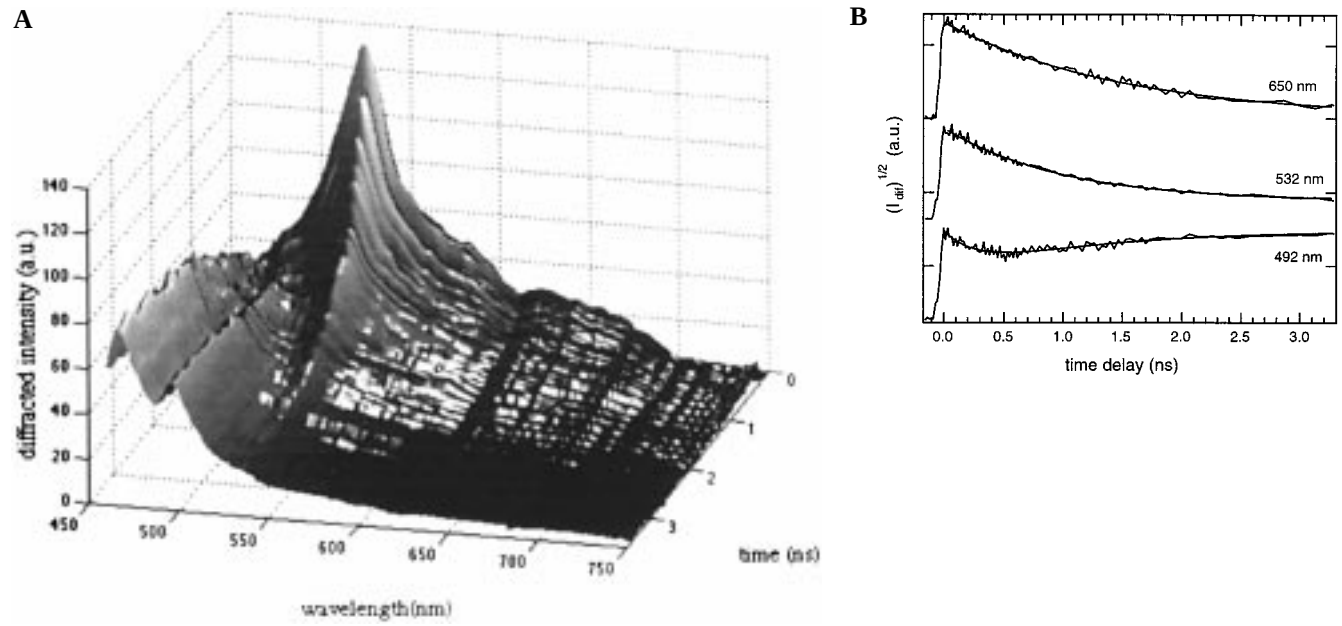

Figure 3. (A) Time-resolved TG spectrum measured with a solution of BP and 0.1 M 1-MONAP in MeCN. (B) Normalized time profiles of the square root of the diffracted intensity at three wavelengths and best single (at 650 and 532 nm) and double (at 492 nm) exponential fits.

Agmon and Levine expression for determining the activation barrier for TT.[11] In this case as well, the rise of the observed yield is shifted toward higher exergonicity, its position corresponding to the free energy at which TT becomes more exergonic than ET.

The relative product yield, ϕ_{ion}/ϕ_T, is either larger than 4 or smaller than 1/4. If the product distribution is kinetically controlled, this indicates that ET quenching is either much faster or much slower than TT quenching. However, cases where both quenching processes are equally fast and where the relative product yield is around unity should have been observed. As this is not the case, the product distribution appears to be rather thermodynamically controlled, i.e., the product is almost exclusively that with the lowest energy.

This observation does not imply that competition between ET and TT does not occur. The final product distribution could depend on interconversion between the ET and TT products, formed directly after the initial triplet quenching, and could therefore be different from the primary product distribution, which reflects the actual competition.

Ps Transient Grating and μs Transient Absorption Measurements. To detect the occurrence of such interconversion, the dynamics of the triplet quenching was investigated using picosecond TG spectroscopy. The nature of a TG spectrum has been discussed in details elsewhere.[21,28] In brief, the diffracted intensity being proportional to the square of the photoinduced changes of absorbance and refractive index,[29] the TG spectrum is the sum of the squares of the absorption and dispersion spectra. The contribution of dispersion to the spectrum leads to a broadening of the TG bands. This effect is counterbalanced by the band narrowing due to the quadratic dependence of the diffracted intensity on concentration. Consequently, the TG spectrum is very similar to the corresponding absorption spectrum.

(1) Type I Pairs: BP/MONAP, XA/1-MONAP. Figure 3A shows the time-resolved TG spectrum measured with a solution of BP and 0.1 M 1-MONAP in MeCN. At short time delay, the spectrum exhibits an intense band with a maximum around 530 nm and with a broad shoulder on the red side corresponding to ^{3}BP* (ϵ_{max} = 7220 M^{-1} cm^{-1}).[30,31] At longer time delay, this band is replaced by a structured band located below 500 nm, which belongs to ^{3}1-MONAP* [ϵ(490 nm) = 3000 M^{-1} cm^{-1}].[32] The radical cation 1-MONAP$^{\cdot+}$ has a broad absorption band with a maximum at 650 nm and with an extinction coefficient of 3400 M^{-1} cm^{-1}.[32,33] To extract the population kinetics from the time-resolved TG spectrum, the square root of the diffracted intensity has to be considered (see Figure 3B). The kinetics at 532 nm, due to ^{3}BP* only, and at 650 nm, due to ^{3}BP* and possibly to 1-MONAP$^{\cdot+}$, are identical within the error limit [k(532 nm) = k(650 nm) = 0.9 $\times$ 10^9 s^{-1}]. This seems to preclude the occurrence of ET between ^{3}BP* and 1-MONAP and indicates that TT essentially takes place through the Dexter mechanism. However a close inspection of the kinetics at 492 nm, where the extinction coefficients of ^{3}BP* and ^{3}1-MONAP* are about the same, reveals the presence of a small dip in the time evolution of the diffracted intensity. This dip, which is also visible, but weaker, with 2-MONAP, indicates that the kinetics of ^{3}MONAP* formation is not identical to the kinetics of ^{3}BP* decay. This could be explained with a reaction scheme where ^{3}MONAP* is partially formed via an indirect route and not exclusively through the direct Dexter mechanism. Tables 1 and 2 show that ET between BP and 1- and 2-MONAP are slightly endergonic. However, the presence of free ions indicates that ET takes place. ET quenching rate constants of the order of 1 $\times$ 10^9 M^{-1} s^{-1} at $\Delta G_{ET} \approx$0.1 eV have been measured with BP and weak donors with a high-lying triplet state.[34] In the same way, Kochi and co-workers have reported that the ET quenching of triplet quinones by aromatic donors with ΔG_{ET} > 0.1 eV was close to the diffusion limit.[35]

The occurrence of an indirect route for the formation of the TT product is more evident with the XA/1-MONAP pair, for which ET quenching is more exergonic. Figure 4A shows the time-resolved TG spectrum measured with XA and 0.1 M 1-MONAP in MeCN. At short time delay (Figure 4B), the TG spectrum exhibits a broad band with maxima around 600 and 650 nm. This band is almost identical to the TG spectrum of ^{3}XA* measured independently and shown in Figure 5. ^{3}XA* is known to have such a broad absorption band centered at 610 nm with an extinction of about 5300 M^{-1} cm^{-1}.[36] As the time delay becomes larger, the spectrum changes to a band with a

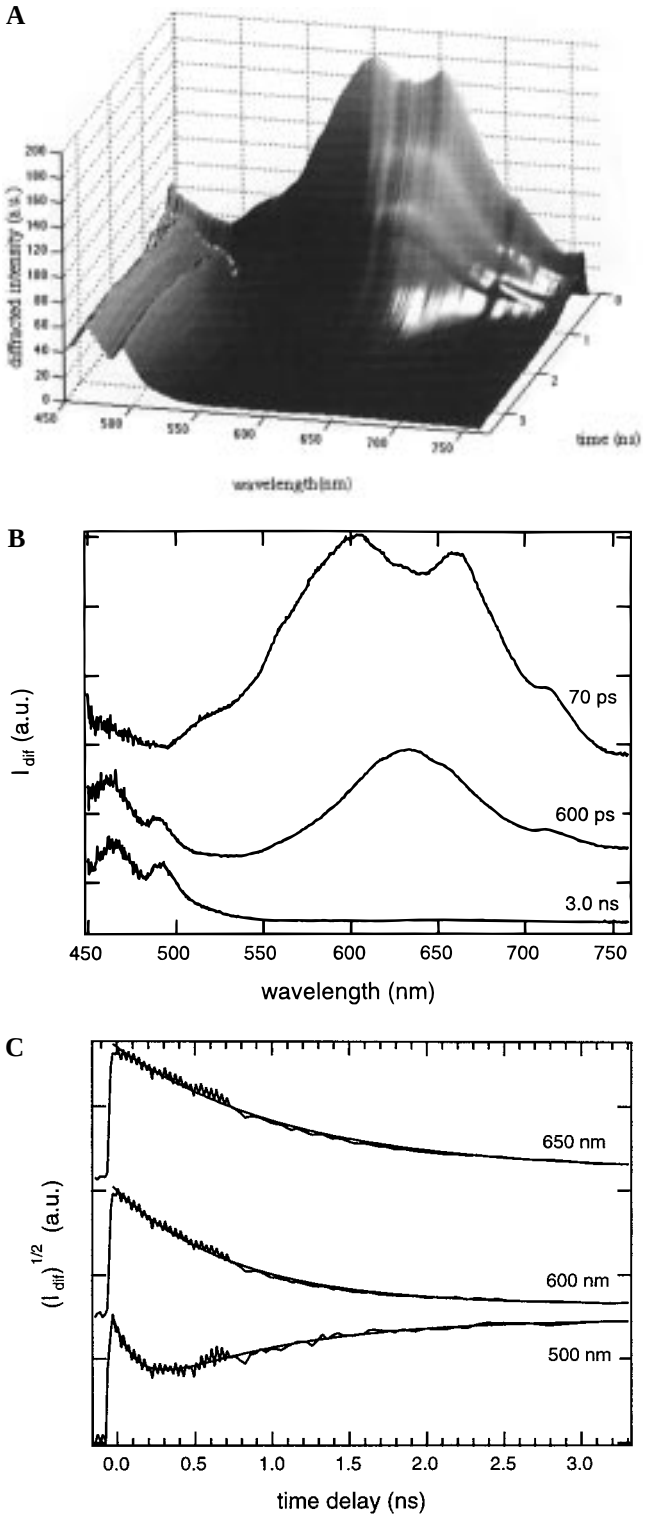

Figure 4. (A) Time-resolved TG spectrum measured with a solution of XA and 0.1 M 1-MONAP in MeCN. (B) TG spectra at various time delays. (C) Normalized time profiles of the square root of the diffracted intensity at three wavelengths and best single (at 650 and 600 nm) and double (at 500 nm) exponential fits.

single maximum around 650 nm. Simultaneously, the structured band of ^{3}1-MONAP* appears.[37] The changes around 650 nm can be explained by a decrease of ^{3}XA* concentration together with the appearance of $XA^{\cdot-}$ and 1-$MONAP^{\cdot+}$. The absorption spectrum of $XA^{\cdot-}$ in neat diethylaniline consists of a broad band around 700 nm.[38] With the system XA/DMA in MeCN, for which an ion yield of 80% has been measured, the time-resolved TG spectrum shows that bands at 475 and 670 nm are formed after the decay of ^{3}XA*. The first one is due to $DMA^{\cdot+}$[39] and consequently, the second one, with an extinction coefficient of the order of 3000 M^{-1} cm^{-1}, can be ascribed to $XA^{\cdot-}$ (see Figure 5).

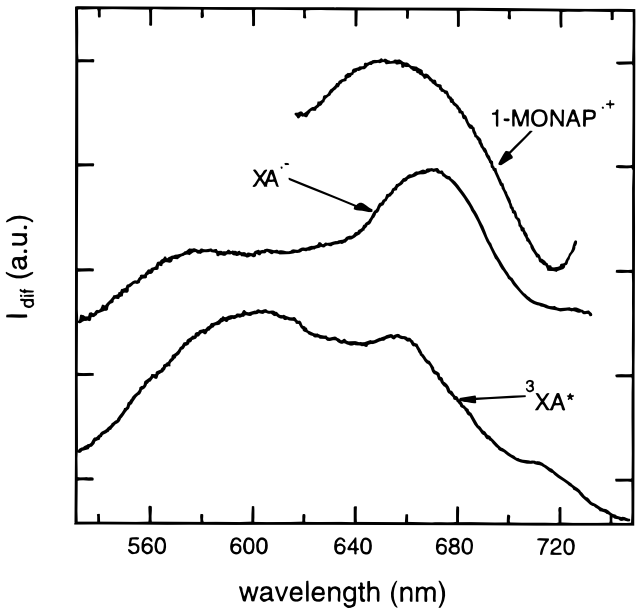

Figure 5. TG spectra of ^{3}XA* in MeCN (bottom), of $XA^{\cdot-}$ obtained by photoinduced ET with DMA (middle) and of 1-MONAP obtained by photoinduced ET with AQ (top).

At much longer time delay, the 650 nm band has almost vanished and the TG spectrum is essentially that of ^{3}1-MONAP*.[37] Figure 4C shows the TG kinetics of the 650 nm band, of ^{3}XA* alone at 600 nm, together with the time profile at 500 nm where both ^{3}XA* and ^{3}1-MONAP* have about the same extinction coefficient. The decay of $I_{dif}^{1/2}$ at 600 nm is monoexponential with a rate constant of 1.5×10^9 s^{-1}. This corresponds to a second-order rate constant for the quenching of ^{3}XA* of 1.5×10^{10} M^{-1} s^{-1}, close to the diffusional limit in MeCN. At 650 nm, the decay is somewhat slower [k(650 nm) $= 1.0 \times 10^9$ s^{-1}] and the single-exponential fit is not as satisfactory. At 500 nm, a dip similar to that measured with BP/1-MONAP but more pronounced can be observed. These time profiles confirm the occurrence of an indirect route from ^{3}XA* to ^{3}1-MONAP. Moreover, the TG spectra indicate that this mechanism involves the formation of the ET product, the triplet geminate ion pair, which then decays to the TT product by spin-allowed BET.

The dip in the time profile at 500 nm reflects the dynamics of the ET product population. The slow rise of the time profile reaches a constant intensity which is slightly smaller than the maximum initial intensity. This intensity difference corresponds to the ion-pair population which has dissociated into free ions and which did not undergo BET to the TT product. This dip was fitted using a two-exponential function, one for the initial decay and one for the slower rise. This procedure was repeated on 10 time profiles between 495 and 505 nm. The resulting rate constants are $k_f = 4.8 \times 10^9$ s^{-1} for the fast initial decay and $k_s = 1.5 \times 10^9$ s^{-1} for the slower rise. The latter rate constant is identical to that determined from the decay of ^{3}XA* at 600 nm, hence k_f must correspond to the decay of the geminate ion pair. In the case of exciplex emission dynamics, it is indeed known that when the exciplex decays faster than it is produced, the time constant for the growth emission component is equal to the exciplex lifetime, while the time constant

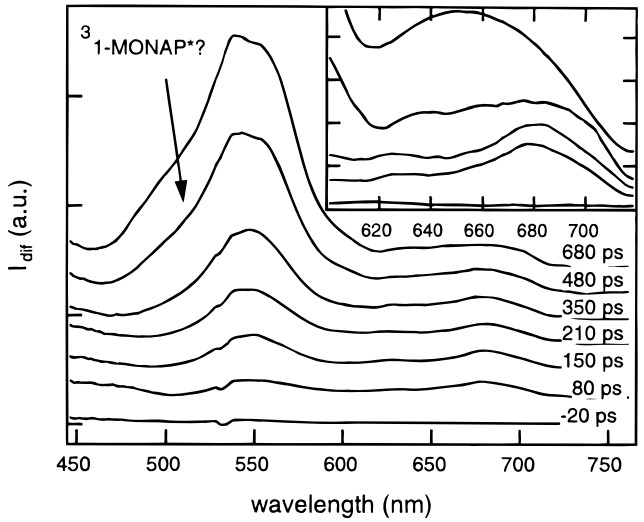

Figure 6. TG spectra at various time delays measured with a solution of AQ and 0.1 M 1-MONAP in MeCN. Inset: magnification of the TG spectra between 600 and 720 nm (from bottom to top: $\Delta t = -20$ ps, 80 ps, 210 ps, 680 ps, and 3.2 ns).

for the decay component is equal to the time constant for exciplex formation.[40] The situation is the same here, because the intermediate decays faster than it is produced. If this fit is also performed on the square root of the time profiles measured around 490 nm with BP/1-MONAP, rate constants of $k_f = 3.4 \times 10^9$ s^{-1} and $k_s = 0.9 \times 10^9$ s^{-1} are obtained. The latter rate constant is the same as that obtained from the decay of ^{3}BP* at 532 nm. With BP/2-MONAP, the fit indicates rate constants of $k_f = 3.1 \times 10^9$ s^{-1} and $k_s = 0.7 \times 10^9$ s^{-1}, the triplet quenching constant being also equal to 0.7×10^9 s^{-1} at 0.1 M 2-MONAP concentration.

(2) Type II Pairs: AQ/MONAP. We consider now systems where ET is more exergonic than TT to see whether the ET product can also be formed via the TT product.

Figure 6 shows the TG spectra measured with AQ and 0.1 M 1-MONAP in MeCN. At short time delay, the spectrum exhibits three weak bands at 677, 619, and around 580 nm which can be ascribed to ^{3}AQ*.[41,42] At longer time delay, a strong band at 540 nm due to AQ$^{\cdot-}$ appears.[39] Simultaneously, a broad band centered at 650 nm and corresponding to 1-MONAP$^{\cdot+}$ develops.[33,37] The weakness of the 1-MONAP$^{\cdot+}$ band is due to its small extinction coefficient relative to that of AQ$^{\cdot-}$ ($\epsilon_{max} \approx 8000$ M^{-1} cm^{-1}) and to the quadratic dependence of the TG intensity on concentration changes. The structured band of ^{3}1-MONAP* cannot be observed. This can be due to the low triplet yield and to the small extinction coefficient of ^{3}1-MONAP*. However, a close inspection on the blue side of the AQ$^{\cdot-}$ band reveals a shoulder which is more pronounced than that observed with other quencher molecules. The kinetics at 540 nm (AQ$^{\cdot-}$), 660 nm (1-MONAP$^{\cdot+}$), and at 500 nm (^{3}1-MONAP*) are identical with a build-up rate constant of 1.9×10^9 s^{-1}. To confirm that the intensity at 500 nm is not due to AQ$^{\cdot-}$ alone, its kinetics was measured in the microsecond time scale by transient absorption. Figure 7A shows time-resolved absorption spectra measured with AQ and 0.1 M 1-MONAP in MeCN. All the bands observed in the TG spectrum can also be seen. Moreover, weak bands which can be due to ^{3}1-MONAP* can be distinguished. Figure 7B shows the kinetics at 560 nm (AQ$^{\cdot-}$) and at 490 nm. The decays at 560 and 650 nm are identical and follow a second-order kinetics, as expected for homogeneous free ion recombination. At 490 nm, the decay is different and follows neither a second-order nor a first-order

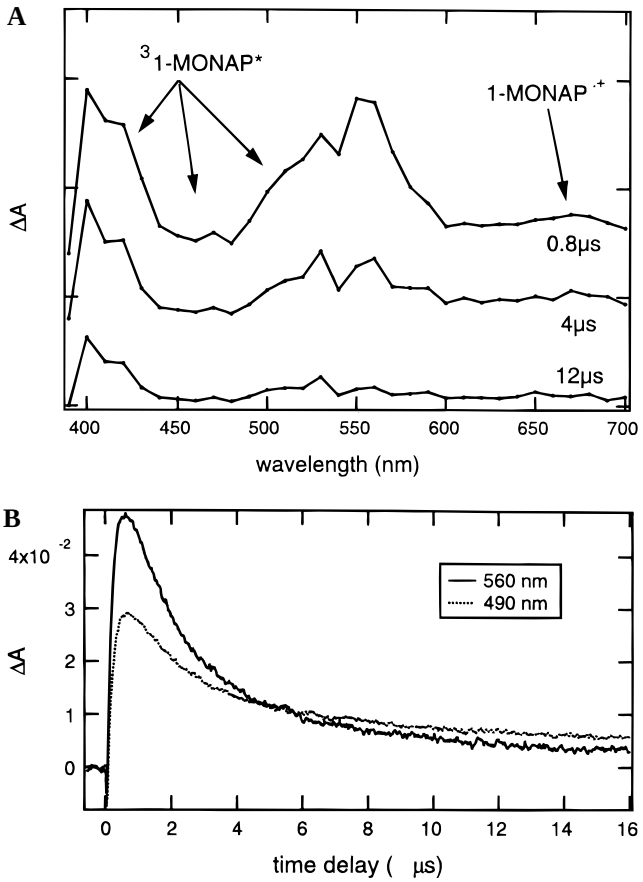

Figure 7. (A) Reconstructed transient absorption spectra at various time delays measured with a solution of AQ and 0.1 M 1-MONAP in MeCN. (B) Microsecond time dependence of the absorbance changes at 490 and 560 nm with the same solution as in (A).

kinetics. This confirms that the absorbance at this wavelength is due not only to AQ$^{\cdot-}$ but also to another species, which must be ^{3}1-MONAP*. Considering the large concentration of 1-MONAP in the ground state, ^{3}1-MONAP* can be expected to decay via concentration quenching and therefore to follow a pseudo-first-order kinetics. This explains the complex decay of the transient absorbance at 490 nm.

Table 2 and Figure 2A show that the free ion yield with NAP and MNAP is substantially lower than expected from the relative free energies of ET and TT. This is due to the occurrence of an additional process. Figure 8 shows TG spectra measured with AQ/MNAP in MeCN at various time delays after excitation. At short time delay, the spectrum is essentially due to ^{3}AQ*. At longer time delay, bands due to AQ$^{\cdot-}$ at 540 nm and MNAP$^{\cdot+}$ between 650 and 700 nm become visible. Another band at 630 nm, with the same kinetics of formation as AQ$^{\cdot-}$ and MNAP$^{\cdot+}$ can be observed. At even longer time delay, the MNAP$^{\cdot+}$ band decays and the red side of the AQ$^{\cdot-}$ band becomes broader. This effect is due to the reaction of MNAP$^{\cdot+}$ with a neutral MNAP molecule to generate the dimer cation, (MNAP$_2$)$^{\cdot+}$. This process has been investigated in details in ref 43. Such a dimerization was not observed with MONAP$^{\cdot+}$. The 630 nm band might be due to AQH$\cdot$ formed by direct atom transfer from MNAP to ^{3}AQ* or by proton transfer within the geminate ion pair generated by ET quenching. Such a two-step atom transfer is known to take place with benzophenone and tertiary amines in MeCN.[44] Carlson and Hercules have reported that the transient absorption spectrum of AQH$\cdot$ in ethanol shows three bands at 678, 631, and 575 nm.[45] In the TG spectrum, the 678 and 575 nm bands could

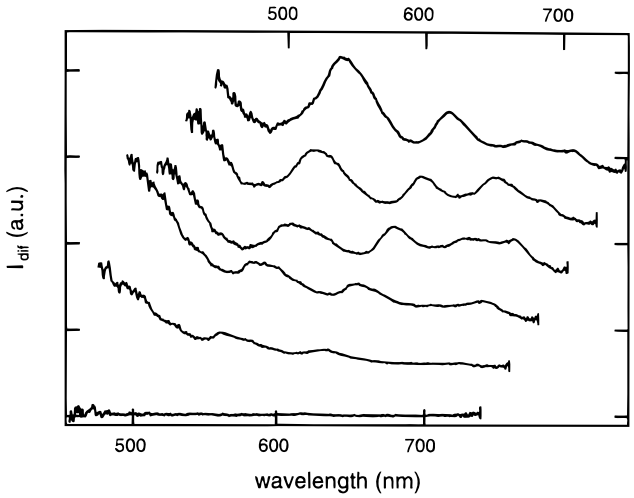

Figure 8. TG spectra measured at various time delays with AQ and 0.1 M MNAP in MeCN (from bottom to top: $\Delta t = -20$ ps, 0 ps, 60 ps, 80 ps, 100 ps, and 500 ps).

be hidden by other more intense bands. Similar TG spectra were obtain with AQ/NAP. These two systems were not further investigated, the competition with a third reaction being beyond the scope of the present study.

Discussion

The above results indicate that for Type I pairs, the TT product can be formed via a two-step mechanism. In principle, the magnitude of the dip observed in the time profile of the diffracted intensity with these pairs can be used to estimate whether the TT product is generated via the two-step mechanism only or additionally through the Dexter mechanism. From computer simulation, using the experimentally determined rate constants, the magnitude of the dip with XA/1-MONAP should amount to 30% of the maximum intensity if quenching occurs through ET only. However, this depth is not very sensitive to the relative efficiency of both processes, as it decreases to 20% if both routes have the same efficiency. These figures are only valid at a wavelength where both ^{3}BP* or ^{3}XA* and ^{3}1-MONAP* have exactly the same extinction coefficient and where there is no contribution of the ET product. If this is not the case, the rate constants are not affected but the magnitude of the dip is influenced. For XA/1-MONAP, the dip was as large as that mentioned above for ET quenching only. For this M/Q pair, the two-step mechanism is therefore the dominant pathway to the TT product. For the BP/MONAP pairs, the dip was substantially smaller than that simulated for ET quenching only. This is not surprising in view of the endergonicity of ET. In this case, the TT product seems to be formed through both Dexter TT and sequential ET.

When both processes are exergonic, as for XA/1-MONAP, ET is apparently more efficient than TT. ET quenching requires a non-zero overlap between the HOMOs of both the electron acceptor (M) and the electron donor (Q). For TT quenching, a non-zero overlap between both the LUMOs of the triplet energy donor (M) and the triplet energy acceptor (Q) is additionally needed. Such an overlap implies a more precise relative geometry of the reaction partners than for ET. Consequently, the reaction distance for ET can be expected to be larger than for TT.

The geminate ion pair decays by both BET to the TT product and separation into free ions. BET to the neutral ground state can be neglected, since it is spin forbidden. If the efficiency of ion pair formation, ϕ_{IP}, is known, the rate constants of separation of the geminate ion pair to free ions, k_{sep}, and the rate constant for BET to the TT product, k_{BET}^{TT}, can be determined from the free ion yield:

$$\Phi_{ion} = \Phi_{IP} = \frac{k_{sep}}{k_{sep} + k_{BET}^{TT}} = \Phi_{IP}\frac{k_{sep}}{k_f} \qquad (5)$$

where k_f is the rate constant for the fast component obtained from the analysis of the time profiles around 500 nm and corresponding to the decay rate constant of the geminate ion pair as discussed above. For XA/1-MONAP, ϕ_{IP} can be reasonably taken as 100%, but for the other two systems, ϕ_{IP} is smaller. The resulting rate constants are listed in Table 3. The k_{sep} value for XA/1-MONAP is of the same order of magnitude as those reported for ion pair dissociation in MeCN.[44,46] One could therefore expect a similar value for the other two pairs. However, a decrease of k_{sep} with decreasing ET exergonicity was recently observed with singlet ion pairs in MeCN.[47] This was explained by a decrease of the charge-transfer character of the quenching product, an exciplex, with decreasing exergonicity. The same effect might be operative here, but the formation of a triplet exciplex is difficult to prove, as this species does not luminesce and as its absorption spectrum contains contributions of both the triplet state and ions.

TABLE 3: Charge Recombination Parameters for Type I Pairs

M/Q pair	BP/1-MONAP	BP/2-MONAP	XA/1-MONAP
ΔG_{ET} (eV)	0.11	0.14	−0.17
ΔG_{BET}^{TT} (eV)	−0.43	−0.55	−0.35
k_q (M^{-1} s^{-1})	9×10^9	7×10^9	15×10^9
Φ_{ion} (%)	7	4	12
Φ_{IP} (%)	<100	<100	100
k_{sep} (s^{-1})	$>2.4 \times 10^8$	$>1.2 \times 10^8$	5.8×10^8
k_{BET}^{TT} (s^{-1})	$<3.2 \times 10^9$	$<3 \times 10^9$	4.2×10^9

According to Marcus theory and considering the magnitude of ΔG_{BET}^{TT}, BET to the TT product should take place in the free energy region where k_{BET}^{TT} increases with increasing exergonicity. Using $\lambda = 1.5$ eV for the total reorganization energy and $V = 10$ cm^{-1} for the electronic coupling matrix element, as determined from the Marcus analysis of BET rate constants within singlet geminate ion pairs,[48,49] k_{BET}^{TT} should be of the order of 3×10^7 s^{-1} for BP/MONAP and 4×10^6 s^{-1} for XA/1-MONAP. If k_{BET}^{TT} was really as low, the separation efficiency of the ion pair should be unity and the contribution of 1-MONAP$^{\cdot+}$ and XA$^{\cdot-}$ to the TG spectrum in Figure 4A should not decay. With the above Marcus parameters, the k_{BET}^{TT} value determined for XA/1-MONAP is obtained with a ΔG_{BET}^{TT} of −0.9 eV. Better agreement can also be obtained with a lower reorganization energy ($\lambda = 0.5$ eV) and/or a larger coupling constant ($V = 300$ cm^{-1}). It is however difficult to find reasonable explanations for a more negative ΔG_{BET}^{TT} value, for a lower λ or for a larger V, although the latter two parameters might vary slightly from one pair to the other. A possible explanation for this discrepancy is that the ET quenching product is not a true geminate ion pair, but rather a triplet exciplex with a charge-transfer character below unity. In this case, charge recombination can no longer be discussed in terms of the Marcus theory.

The data obtained with Type II pairs show no evidence for the conversion of the TT product to the ET product. The same behavior was observed with the system AQ/2-MONAP. If some conversion takes place, its efficiency must be rather low in view

of the relatively large triplet yield. This is not surprising if one considers that the conversion from TT to ET product requires contact or at least a short distance between the reaction partners. Such a condition exists either directly after TT, while AQ and ^{3}MONAP* are still in contact, or after a diffusional encounter between ^{3}MONAP* and AQ. Considering that the AQ concentration is smaller than 1×10^{-3} M, diffusional encounter with ^{3}MONAP* is very slow. Therefore an efficient conversion can only take place directly after TT. The diffusion of the TT product molecules is much faster than that of geminate ions, since there is no electrostatic interaction. The corresponding rate constant must be typically of the order of 1×10^{10} s^{-1} in MeCN, and therefore if conversion takes place, its rate constant has to be of this order of magnitude as well. The kinetics at 680 nm, where the extinction coefficients of ^{3}AQ* and 1-MONAP$^{\cdot+}$ are approximately the same, does not exhibit any dip which could indicate that the formation of MONAP$^{\cdot+}$ from ^{3}AQ* does not occur through a single step process only. As the TG signal at this wavelength is weak, a dip with a magnitude of less than 10% of the maximum diffracted intensity cannot be observed accurately. Computer simulation shows that if the initial triplet yield is 50%, the rate constant for TT to ET product conversion should be larger than 3×10^{10} s^{-1} to have a dip shallower than 10%. Considering that the final triplet yield is around 25%, this implies that the rate constant for the diffusion of the TT product molecules must be as large as 3×10^{10} s^{-1}, which is not totally unrealistic. Consequently, this reaction channel to the ET product cannot be ruled out. However if this was the dominant channel, the triplet yield would be even smaller, of the same order of magnitude as the ion yield measured for systems where conversion from ET to TT product is operative. Thus, the final product distribution reflects essentially the primary product distribution. As mentioned above, orbital overlap favors ET relative to TT. However, ET is strongly solvent dependent, contrary to TT. If both reactions are energetically feasible, solvent fluctuation could favor one process over the other.

Summary and Conclusion

This investigation shows that when both ET and TT are energetically feasible, the product distribution observed in the microsecond time scale depends strongly on the relative free energies of the two processes. The product with the lowest energy is at least four times more abundant than the other. However, the picosecond measurements show that the final product distribution is not the same as the primary product distribution, i.e., that just after the excited state quenching. When TT is more exergonic than ET, there is clear evidence that the TT product is dominantly formed via the ET product, i.e., through a sequential double ET. In this case, the free ion yield is much lower than the efficiency of the geminate ion pair formation. Similarly, the final triplet yield is much larger than the efficiency of the Dexter TT. The reason for the higher efficiency of ET quenching compared with TT quenching in polar solvents can be explained by the severe overlap requirements for the exchange mechanism. This difference should result in a shorter reaction distance for TT than for ET. In these circumstances, the Dexter TT cannot be univocally invoked to explain the presence of TT product on the microsecond time scale. When TT is less exergonic than ET, no conversion of the TT product to the ET product could be observed. The final product distribution is apparently the same as the initial one. In this case, the low triplet yield is essentially due to the competition between ET and TT and, as discussed above, ET is favored. ET is faster, as long as both ET and TT are weakly to moderately exergonic. However, if ET was highly exothermic, it might become slower than TT.

Acknowledgment. This work was supported by the Fonds national suisse de la recherche scientifique through project number 20-49235.96 and by the program d′encouragement à la relève universitaire de la Confédération. Financial support from the Fonds de la recherche and the Conseil de l′Université de Fribourg is also acknowledged.

References and Notes

(1) Förster, T. *Ann. Physik* **1948**, *2*, 55.
(2) Dexter, D. L. *J. Chem. Phys* **1953**, *21*, 836.
(3) Closs, G. L.; Johnson, M. D.; Miller, J. R.; Piotrowiak, P. *J. Am. Chem. Soc.* **1989**, *111*, 3751.
(4) Closs, G. L.; Piotrowak, D.; MacInnis, J.; Fleming, J. R. *J. Am. Chem. Soc.* **1988**, *110*, 2652.
(5) Knibbe, H.; Rehm, D.; Weller, A. *Ber. Bunsen-Ges.* **1968**, *72*, 257.
(6) Weller, A.; Rehm, D. *Ber. Bunsen-Ges.* **1969**, *73*, 834.
(7) Rehm, D.; Weller, A. *Isr. J. Chem.* **1970**, *8*, 259.
(8) Wilkinson, F. *Pure Appl. Chem.* **1975**, *41*, 661.
(9) Scandola, F.; Balzani, V. *J. Chem. Educ.* **1983**, *60*, 814.
(10) Marciniak, B.; Hug, G. L. *Coord. Chem. Rev.* **1997**, *159*, 55.
(11) Agmon, N.; Levine, R. D. *Chem. Phys. Lett.* **1977**, *52*, 197.
(12) Closs, G. L.; Miller, J. R. *Sciences* **1988**, *240*, 440.
(13) Wasielewski, M. R.; Niemczyk, N. P.; Svec, W. A.; Pewitt, E. B. *J. Am. Chem. Soc.* **1985**, *107*, 1080.
(14) Sigman, M. E.; Closs, G. L. *J. Phys. Chem.* **1991**, *95*, 5012.
(15) MacQueen, D. B.; Eyler, J. R.; Schanze, K. S. *J. Am. Chem. Soc.* **1992**, *114*, 1897.
(16) Farran, A.; Deshayes, K. D. *J. Phys. Chem.* **1996**, *100*, 3305.
(17) Kiyota, T.; Yamaji, M.; Shizuka, H. *J. Phys. Chem.* **1996**, *100*, 672.
(18) Yamaji, N.; Kiyota, K.; Shizuka, H. *Chem. Phys. Lett.* **1994**, *226*, 199.
(19) Tinkler, J. H.; Tavender, S. M.; Parker, A. W.; McGarvey, D. J.; Mulroy, L.; Truscott, T. G. *J. Am. Chem. Soc.* **1996**, *118*, 1756.
(20) Fournier, T.; Tavender, S. M.; Parker, A. W.; Scholes, G. D.; Phillips, D. *J. Phys. Chem. A* **1997**, *101*, 5320.
(21) Högemann, C.; Pauchard, M.; Vauthey, E. *Rev. Sci. Instrum.* **1996**, *67*, 3449.
(22) von Raumer, M.; Suppan, P.; Jacques, P. *J. Photochem. Photobiol. A* **1997**, *105*, 21.
(23) Henseler, A.; Vauthey, E. *J. Photochem. Photobiol. A* **1995**, *91*, 7.
(24) Vauthey, E.; Pilloud, D.; Haselbach, E.; Suppan, P.; Jacques, P. *Chem. Phys. Lett.* **1993**, *215*, 264.
(25) Carmichael, I.; Hug, G. L. *J. Phys. Chem. Ref. Data* **1986**, *15*, 1.
(26) Haselbach, E.; Vauthey, E.; Suppan, P. *Tetrahedron* **1988**, *44*, 7335.
(27) Haselbach, E.; Jacques, P.; Pilloud, D.; Suppan, P.; Vauthey, E. *J. Phys. Chem.* **1991**, *95*, 7115.
(28) Fayer, M. D. *Annu. Rev. Phys. Chem.* **1982**, *33*, 63.
(29) Kogelnik, H. *Bell. Syst. Technol. J.* **1969**, *48*, 2909.
(30) Godfrey, T. S.; Hilper, J. W.; Porter, G. *Chem. Phys. Lett.* **1967**, *1*, 490.
(31) Miyasaka, H.; Morita, K.; Kamada, K.; Mataga, N. *Chem. Phys. Lett.* **1991**, *178*, 504.
(32) Shizuka, H. *Pure Appl. Chem.* **1997**, *69*, 825.
(33) Johnston, L. J.; Kanigan, T. *J. Am. Chem. Soc.* **1990**, *112*, 1271.
(34) von Raumer, M. Ph.D. Thesis, University of Fribourg, 1996.
(35) Rathore, R.; Hubig, S. M.; Kochi, J. K. *J. Am. Chem. Soc.* **1997**, *119*, 11468.
(36) Abdullah, K. A.; Kemp, T. J. *J. Chem. Soc., Perkin Trans. 2* **1985**, *8*, 610.
(37) Yamaji, M.; Sekiguchi, T.; Hoshino, M.; Shizuka, H. *J. Phys. Chem.* **1992**, *96*, 9353.
(38) Hoshima, M.; Seki, H.; Shizuka, H. *Chem. Phys.* **1989**, *129*, 395.
(39) Shida, T. *Electronic Absorption Spectra of Radical Ions*; Elsevier: Amsterdam, 1988; Vol. Physical Sciences Data 34.
(40) Gould, I. R.; Farid, S. *J. Am. Chem. Soc.* **1993**, *115*, 4814.
(41) Manring, L. E.; Peters, K. S. *J. Am. Chem. Soc.* **1985**, *107*, 6452.
(42) Hamanoue, K.; Nakayama, T.; Yamamoto, Y.; Sawada, K.; Yuhara, Y.; Teranishi, H. *Bull. Chem. Soc. Jpn.* **1988**, *61*, 1121.
(43) Vauthey, E. *J. Phys. Chem. A* **1997**, *101*, 1635.
(44) Miyasaka, H.; Nagata, T.; Kiri, M.; Mataga, N. *J. Phys. Chem.* **1992**, *96*, 8060.
(45) Carlson, S. A.; Hercules, D. M. *Photochem. Photobiol.* **1973**, *17*, 123.

(46) Mataga, N.; Asahi, T.; Kanda, Y.; Okada, T.; Kakitani, T. *Chem. Phys.* **1988**, *127*, 249.
(47) Vauthey, E.; Allonas, X.; Högemann, C. *J. Phys. Chem. A* **1998**, *102*, 7362.
(48) Gould, I. R.; Ege, D.; Moser, J. E.; Farid, S. *J. Am. Chem. Soc.* **1990**, *112*, 4290.
(49) Vauthey, E.; Suppan, P.; Haselbach, E. *Helv. Chim. Acta* **1988**, *71*, 93.
(50) Murov, S. L. *Handbook of Photochemistry*; M. Dekker: New York, 1973.
(51) Weinberg, N. L.; Weinberg, H. R. *Chem. Rev.* **1968**, *68*, 449.
(52) Guttenplan, J. B.; Cohen, S. B. *J. Am. Chem. Soc.* **1972**, *94*, 4040.
(53) Bonafede, S.; Ciano, M.; Bolletta, F.; Balzani, V.; Chassot, L.; von Zelewsky, A. *J. Phys. Chem.* **1986**, *90*, 3836.
(54) Peover, M. E. *J. Chem. Soc.* **1962**, 4541.
(55) Pilloud, D. PhD Thesis, University of Fribourg, 1993.